ORIGINAL RESEARCH

Postnatal Hyperoxia Exposure Durably Impairs Right Ventricular Function and Mitochondrial Biogenesis

Kara N. Goss[1,2], Santosh Kumari[1,2], Laura H. Tetri[2,3], Greg Barton[2,3], Rudolf K. Braun[2,3], Timothy A. Hacker[4], and Marlowe W. Eldridge[2,3]

[1]Division of Allergy, Pulmonary and Critical Care Medicine, Department of Medicine, [3]Division of Pediatric Critical Care, Department of Pediatrics, [2]Rankin Laboratory of Pulmonary Medicine, and [4]Cardiovascular Research Center, Department of Medicine, University of Wisconsin School of Medicine and Public Health, Madison, Wisconsin

Abstract

Prematurity complicates 12% of births, and young adults with a history of prematurity are at risk to develop right ventricular (RV) hypertrophy and impairment. The long-term risk for pulmonary vascular disease, as well as mechanisms of RV dysfunction and ventricular–vascular uncoupling after prematurity, remain poorly defined. Using an established model of prematurity-related lung disease, pups from timed-pregnant Sprague Dawley rats were randomized to normoxia or hyperoxia (fraction of inspired oxygen, 0.85) exposure for the first 14 days of life. After aging to 1 year in standard conditions, rats underwent hemodynamic assessment followed by tissue harvest for biochemical and histological evaluation. Aged hyperoxia-exposed rats developed significantly greater RV hypertrophy, associated with a 40% increase in RV systolic pressures. Although cardiac index was similar, hyperoxia-exposed rats demonstrated a reduced RV ejection fraction and significant RV–pulmonary vascular uncoupling. Hyperoxia-exposed RV cardiomyocytes demonstrated evidence of mitochondrial dysregulation and mitochondrial DNA damage, suggesting potential mitochondrial dysfunction as a cause of RV dysfunction. Aged rats exposed to postnatal hyperoxia recapitulate many features of young adults born prematurely, including increased RV hypertrophy and decreased RV ejection fraction. Our data suggest that postnatal hyperoxia exposure results in mitochondrial dysregulation that persists into adulthood with eventual RV dysfunction. Further evaluation of long-term mitochondrial function is warranted in both animal models of premature lung disease and in human adults who were born preterm.

Keywords: pulmonary hypertension; mitochondrial biogenesis; prematurity

Clinical Relevance

This study used a common rat model of chronic lung disease of prematurity aged to 1 year, similar to young adulthood in humans, to study the long-term effects on the right ventricle (RV) and pulmonary vasculature. These rats demonstrated significant RV hypertrophy and dysfunction, similar to human studies, and newly identified significant chronic pulmonary hypertension. In addition, there was evidence of mitochondrial dysregulation in the RV, which may provide new insight into the pathogenesis of RV dysfunction in human adults born prematurely.

Rates of prematurity have steadily increased over the past few decades, now accounting for 10–12% of live births in the United States (1). With improvements in neonatal care and increasing survival of premature infants, the number of adults born premature is also rising. While prematurity is clearly associated with increased risk for pulmonary (2–4), metabolic (5, 6), and systemic cardiovascular disease (7, 8) into adulthood, the long-term implications of prematurity for the right ventricle (RV) and pulmonary vasculature remain poorly defined. A potential role for prematurity in the development of adult pulmonary arterial hypertension has been suggested by a recent registry study (9), though the mechanisms remain unknown. Furthermore, in a landmark study in 2013, Lewandowski and colleagues (8, 10) demonstrated that young adults born preterm exhibit greater RV mass and lower RV ejection fraction than age-matched adults born at term, and these RV changes were significantly greater than changes observed within the left ventricle (LV). However, this study did not evaluate the effect of prematurity on the pulmonary vasculature or RV–pulmonary vascular coupling, making it difficult to identify if prematurity represents a direct insult to the RV independent of the effects of increased afterload and pulmonary hypertension, or rather leads to chronic RV changes as a consequence of the effects of prematurity on the pulmonary vasculature.

Animal models have been used to help characterize the long-term risks of prematurity. In the neonatal rat or mouse born at term, the lung developmental stage at birth is similar to a human infant born in the late second trimester. Postnatal hyperoxia exposure (Hx) in neonatal rodents is frequently used to mimic chronic lung disease of prematurity, also known as bronchopulmonary dysplasia (11). Importantly, the rodent heart is also relatively premature at the time of birth, suggesting that this model may be appropriate to mimic the effects of prematurity on the heart as well (12). Brief neonatal oxygen exposure in mice was previously associated with increased RV hypertrophy, reduced pulmonary microvasculature, and premature death in adulthood (13). Given that the initial injury in these models, and in humans born prematurely, occurs during a period of late cardiopulmonary development, there may be unique RV adaptations and maladaptations to neonatal Hx and chronic pressure overload.

We hypothesized that postnatal Hx results in chronic pulmonary hypertension, RV dysfunction, and decreased efficiency of RV–pulmonary vascular coupling in an aged rat model of chronic lung disease of prematurity, resulting in an increased potential for RV failure later in life. To better understand the risk for RV failure, we also investigated the role of adaptive and maladaptive remodeling responses in contributing to a dysfunctional RV phenotype. Given the known sex differences in RV function in health and disease (14), as well as the propensity for premature male neonates to develop more severe bronchopulmonary dysplasia and pulmonary hypertension (15), a secondary aim was to evaluate sex-specific RV responses after postnatal hyperoxia. Here, we demonstrate a phenotype of RV–pulmonary vascular uncoupling and RV contractile dysfunction in the absence of overt RV failure associated with impaired mitochondrial biogenesis and mitochondrial DNA damage, with changes being most pronounced in hyperoxia-exposed male animals. Some of the results of these studies have been previously reported in the form of an abstract (16).

Materials and Methods

Animal Model

Timed-pregnant Sprague Dawley dams delivered naturally at term. Within 12 hours of birth, male and female newborn pups were pooled and randomized to normoxic exposure (Nx) or Hx. Both groups were housed in standard rat cages within a sealed $30'' \times 20'' \times 20''$ polypropylene chamber with a clear acrylic door (Coy Laboratory, Grass Lake, MI), with continuous oxygen delivery set to achieve 21% fraction of inspired oxygen in the normoxic chamber and 85% fraction of inspired oxygen in the hyperoxic chamber. Dams were rotated between chambers daily to prevent maternal oxygen toxicity. At the end of the 14-day exposure period, all animals were removed from the chambers. Pups were weaned at 21 days. Animals were then allowed to age out to 1 year (~52 wk) in standard animal housing. Animals were allowed access to food and water *ad libitum* throughout the study. All animal protocols were approved by the University of Wisconsin (Madison, WI) Institutional Animal Care and Use Committee.

Echocardiography and Invasive RV Pressure–Volume Loops

Echocardiography and RV pressure–volume loops were performed in the University of Wisconsin Cardiovascular Physiology Core, as previously described (17, 18). Full descriptions of the techniques are available in the online supplement.

Tissue Harvesting and Fixation

After hemodynamic assessment, animals were exsanguinated. The heart was excised and the RV separated from the LV and septum and weighed for calculation of Fulton index. The RV apex was fixed in formalin, embedded in paraffin, and stained with Masson's trichrome for evaluation of fibrosis. Images were taken at 40× with an Olympus BX60 microscope (Olympus, Waltham, MA), and scored qualitatively by two blinded observers for severity of fibrosis. Collagen content was assessed as described in the online supplement. Lungs were inflated and fixed in formaldehyde for vascular analysis, as described in the online supplement.

The remainder of the RV was flash frozen for biochemical assessment or frozen section. Cryosectioned RV was obtained at 7-μm-thick sections and stained with cytochrome c oxidase (COX) and succinate dehydrogenase (SDH) dual staining, as previously described (19), except for an extended incubation time of 1 hour for COX. Images were taken (five images from two to three separate tissue sections per animal, four animals per group) at 40× with an Olympus BX60 microscope. Images were analyzed using a 400-point grid to determine the ratio points overlying COX^-/SDH^+ (COX deficient, *blue*) cardiomyocytes versus COX^+/SDH^+ (*brown*) cardiomyocytes, and data presented as percent COX-deficient cells.

Western Blot, Quantitative Real-Time RT-PCR, and Citrate Synthase Activity

Western blotting using quantitative near-infrared fluorescence (LICOR Imaging System; Lincoln, NE) and quantitative real-time RT-PCR of RV homogenates were

conducted, as previously described (20) and as outlined in the online supplement. Citrate synthase activity assay was performed using a citrate synthase activity colorometric assay kit (Bio-Vision, Inc., Milpitas, CA), per the manufacturer's instructions. Full methods details can be found in the online supplement.

Statistical Analysis

Two-way ANOVA was used to compare normoxia to Hx including analysis of sex differences, with Bonferroni's multiple comparisons test used for analyzing sex-related differences (GraphPad Prism 6; GraphPad Software Inc., San Diego, CA). A P value of less than 0.05 was considered significant.

Results

Rats Exposed to Postnatal Hyperoxia Develop RV Hypertrophy

Postnatal Nx included a total of 16 rats (seven males [Nx-M], nine females [Nx-F]), while 18 rats (nine males [Hx-M], nine females [Hx-F]) underwent postnatal Hx. At 1 year, both Hx-M and Hx-F demonstrated significantly higher body mass compared with Nx-M and Nx-F, respectively (Figure 1A). Hx rats also exhibited significant increases in RV mass, as assessed by Fulton index, and RV mass normalized to body surface area, estimated by the Vallois equation (21), with differences between Nx and Hx being more pronounced in males (Figures 1B and 1C). There were no significant effects of hyperoxia on gross LV mass or LV mass normalized to body surface area (Figure 1D).

Noninvasive hemodynamic assessment by echocardiography identified an increased RV wall thickness in male and female Hx animals (Table 1). An increase in LV wall thickness compared with Nx was only noted in Hx-F (Table 1). Hx also resulted in an increased velocity through both the pulmonic and aortic valves, suggestive of increased pulmonary and systemic pressures or, alternatively, of increased stroke volume and cardiac output (CO). However, aside from expected differences between sexes due to body size, no significant differences were identified in LV ejection fraction, LV fractional shortening, stroke volume, CO, or cardiac index by echocardiograph after Hx (Table 1).
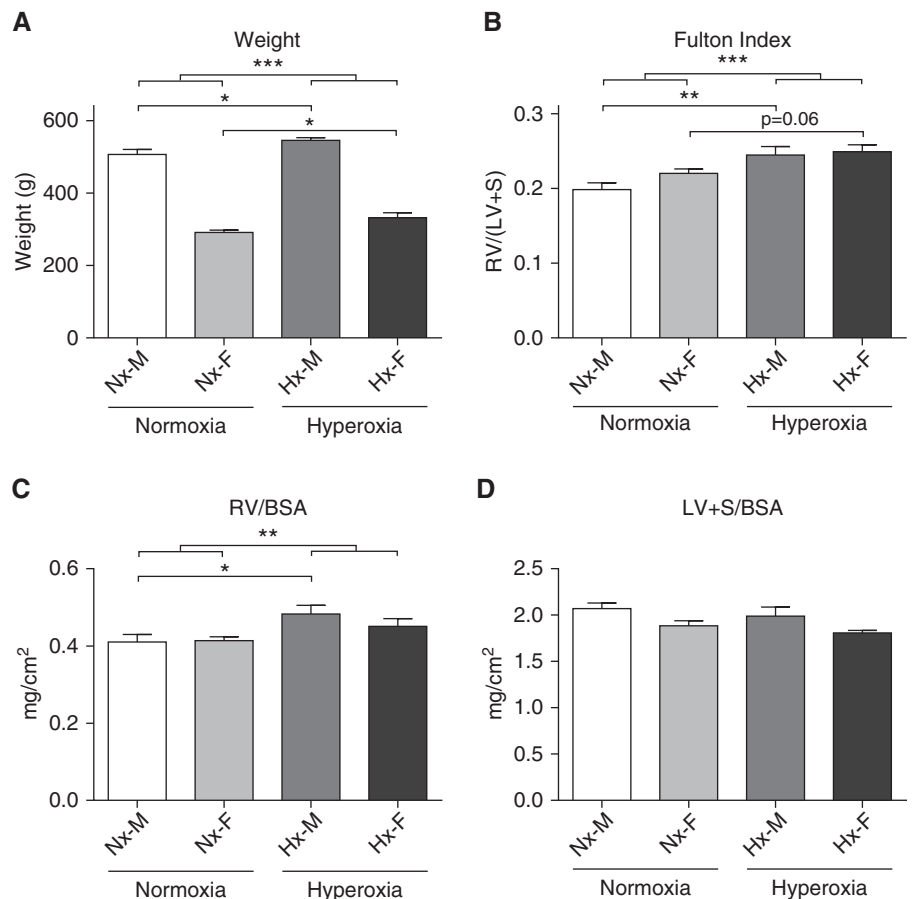

Figure 1. Body weight and right ventricular (RV) weight are increased after postnatal hyperoxia. Postnatal hyperoxia exposure (Hx) is associated with increased body weight (*A*) and RV hypertrophy (*B*) with age. When normalized to body surface area (BSA), RV mass (*C*), but not left ventricular (LV) mass (*D*), was significantly higher. *Error bars*, SEM. Analysis by two-way ANOVA with Bonferroni's multiple comparisons test; $n = 7$–9 per group. F, female; M, male; Nx, normoxia; RV/LV + S, RV to LV plus septum (S) ratio. *$P < 0.05$, **$P < 0.01$, ***$P < 0.001$.

Invasive Hemodynamic Assessment Reveals Significant RV Dysfunction and RV–Pulmonary Vascular Uncoupling with Age after Hyperoxia

Invasive hemodynamic assessment by pressure–volume admittance catheter revealed significant pulmonary hypertension after Hx, particularly in Hx-M, as evidenced by a 59% increase in RV systolic pressure and 64% increase in RV diastolic pressure in Hx-M compared with Nx-M (Figures 2A and 2B). This was associated with increased pulmonary arterial elastance, again present in both Hx sexes, but most pronounced in Hx-M (Figure 2C), suggestive of an increase in RV afterload in Hx animals. To better understand the cause of increased RV afterload and the elevated arterial elastance identified by invasive hemodynamic

assessments, we analyzed pulmonary vascular density by von Willebrand factor staining. Animals exposed to postnatal hyperoxia demonstrated significantly fewer vessels per high-power field compared with controls (*see* Figure E1 in the online supplement), suggesting decreased pulmonary vascular surface area as a cause of pulmonary vascular disease.

Although CO was not different after Hx (Figure 2D), RV cardiac contractility, as measured by the end-systolic pressure–volume relationship was significantly decreased after Hx (Figure 2E), and RV ejection fraction was depressed (Figure 2F). Hx animals also demonstrated evidence of increased diastolic dysfunction, demonstrated by a prolonged relaxation time (Tau;

Table 1. Hemodynamic Variables by Sex and Exposure as Measured by Echocardiography

| Echo Parameter | Normoxia | | Hyperoxia | | *P* Value | | |
	Males (*n* = 7)	Females (*n* = 8)	Males (*n* = 8)	Females (*n* = 9)	Nx versus Hx	Nx-M versus Hx-M	Nx-F versus Hx-F
Heart rate, beats/min	297 ± 14	314 ± 14	319 ± 12	323 ± 11	NS	NS	NS
RV wall thickness, mm	0.76 ± 0.07	0.65 ± 0.06	0.99 ± 0.09	0.93 ± 0.15	0.03	NS	NS
LV anterior wall thickness, mm	1.68 ± 0.04	1.38 ± 0.06	1.67 ± 0.06	1.58 ± 0.02	NS	NS	0.02
Pulmonic valve peak velocity, mm/s	892 ± 43	749 ± 36	1094 ± 71	899 ± 81	0.01	NS	NS
Aortic valve peak velocity, mm/s	876 ± 78	1,085 ± 94	1,163 ± 192	1,265 ± 130	NS	NS	NS
Aortic valve VTI, cm	4.0 ± 0.3	4.4 ± 0.5	5.7 ± 1.0	5.7 ± 0.5	0.03	NS	NS
LV ejection fraction, %	69.3 ± 2.4	77.5 ± 2.1	69.8 ± 3.1	82.6 ± 1.9	NS	NS	NS
LV fractional shortening, %	40.8 ± 2.0	48.2 ± 2.1	41.8 ± 2.6	53.3 ± 2.1	NS	NS	NS
Stroke volume, μl	270.7 ± 17.2	214.1 ± 8.7	297.5 ± 29.3	248.0 ± 21.1	NS	NS	NS
Cardiac output, ml/min	80.18 ± 5.6	67.9 ± 4.8	97.8 ± 10.4	80.5 ± 6.8	NS	NS	NS
Cardiac index, ml/min/g	0.16 ± 0.01	0.23 ± 0.01	0.18 ± 0.02	0.24 ± 0.01	NS	NS	NS

Definition of abbreviations: F, female; Hx, hyperoxia; LV, left ventricle; M, male; NS, not significant; Nx, normoxia; RV, right ventricle; VTI, velocity time integral.
Echocardiography identified RV (both sexes) and LV (females) hypertrophy in hyperoxia-exposed animals. This was associated with a significant increase in pulmonary valve peak velocity and aortic valve VTI after neonatal Hx. However, LV ejection fraction, stroke volume, and cardiac output were maintained after Hx. Results are presented as mean (±SEM). Statistics by two-way ANOVA with Bonferroni's multiple comparisons test.

Figure 2H). The end result was severe ventriculo–vascular uncoupling with age in Hx animals (Figure 2I). Taken together, these data suggest significant RV dysfunction in the absence of overt failure, and an inability of the RV to compensate for the increased afterload in Hx animals.

Gene Profile of Adaptive RV Hypertrophy Maintained after Postnatal Hyperoxia and Chronic RV Pressure Overload

We next sought to better understand what adaptive or maladaptive remodeling responses might contribute to the RV dysfunction seen in this model. A molecular signature of decreased vascular endothelial growth factor (VEGF)-A and apelin, increased hexokinase (HK)-1, decreased alcohol dehydrogenase-7, and stable insulin-like growth factor-1 gene expression has previously been reported in RV failure, with the panel able to differentiate RV failure from the more adaptive RV hypertrophy seen in chronic pressure overload states (22). Surprisingly, the Hx RV did not demonstrate a gene profile consistent with a maladaptive phenotype, despite the degree of RV dysfunction identified on hemodynamic evaluation. Rather, the Hx RV demonstrated increased expression of VEGF-A, decreased HK1, and unchanged alcohol dehydrogenase-7

and insulin-like growth factor-1, more consistent with an adaptive chronic pressure overload state (Figure 3). Given the long-term persistence of these adaptive features, including maintained angiogenesis, as evidenced by increased VEGF-A, as well as absence of a clear glycolytic shift based on decreased HK1, we next evaluated markers of accelerated cardiac aging as an alternate hypothesis to explain the RV dysfunction in this model, including mitochondrial biogenesis, autophagy, and fibrosis.

Postnatal Hyperoxia Results in Impaired Mitochondrial Biogenesis and Mitochondrial DNA Damage with Age

To evaluate for alternative causes of RV decompensation, and given the known importance of mitochondrial function for cardiac homeostasis (23), we assessed RV mitochondrial abundance and dynamics. Aged Hx animals demonstrated an increased abundance of mitochondrial structural proteins, including SDH, COX IV, voltage-dependent anion channel, and heat shock protein 60 (Figures 4A–4E), suggestive of an increase in overall mitochondrial content, as these are frequently used as mitochondrial loading controls (24, 25). These changes were most prominent in Hx-M. Citrate synthase activity was also increased in Hx-M (Figure 4F), again supportive of an

increase in total mitochondrial content. Finally, the ratio of mitochondrial to nuclear DNA was increased in Hx RV, again supportive of an increase in total mitochondrial content (Figure 4G). Surprisingly, despite the evidence of increased mitochondrial abundance in aged Hx animals, there was a significant decrease in transcription of genes associated with mitochondrial biogenesis, including peroxisome proliferator–activated receptor γ coactivator 1α, mitochondrial transcription factor A, and peroxisome proliferator–activated receptor α (Figures 4H–4J).

Dual immunohistochemical staining for SDH and COX in cryosectioned RV demonstrated a robust presence of COX[−]/SDH[+] RV cardiomyocytes after postnatal Hx, with findings again most pronounced in Hx-M (Figures 5A and 5B). As COX is partially encoded by mitochondrial DNA, whereas SDH is nuclear encoded, this pattern of functionally COX-deficient cells is highly suggestive of accumulation of mitochondrial DNA damage at 1 year of age (19, 26). Importantly, mitochondrial DNA deletion mutations that accumulate with age are typically large, involving the major arc with the gene encoding mitochondrially encoded nicotinamide adenine dinucleotide[+] reduced dehydrogenase (ND) 4 routinely deleted, whereas the minor arc
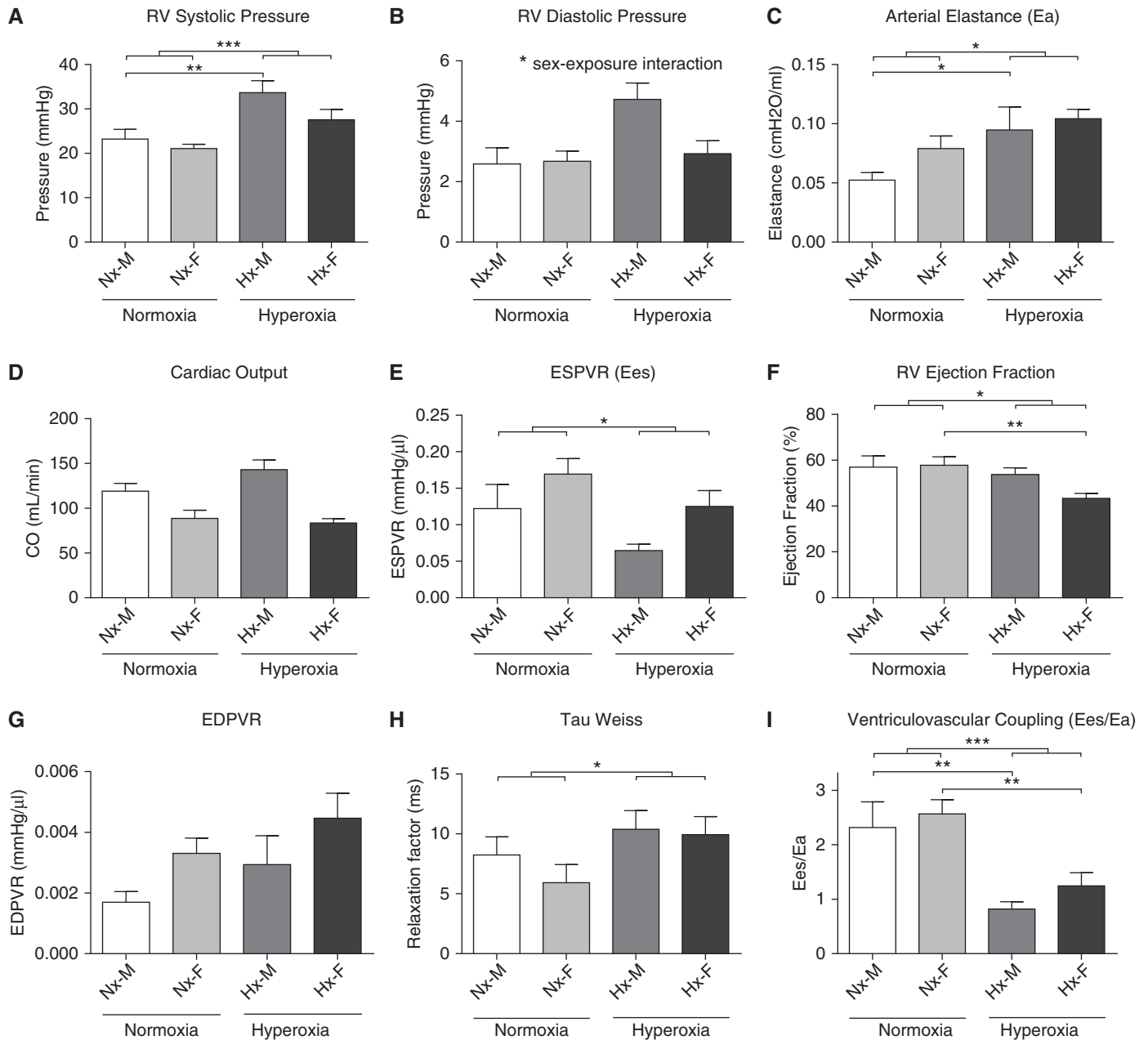
Figure 2. Invasive hemodynamics reveal significant RV dysfunction after Hx. Postnatal Hx is associated with persistent pulmonary hypertension (*A* and *B*) and increased arterial elastance or afterload (*C*) 1 year later. Although cardiac output (CO) is maintained (*D*), RV function is characterized by systolic and diastolic dysfunction, as measured by end-systolic pressure–volume relationship (*E*) and RV ejection fraction (*F*), and EDPVR (G) and Tau Weiss relaxation factor (*H*), respectively. The end result is significant RV–pulmonary vascular uncoupling, as defined by a marked decrease in end-systolic elastance/arterial elastance (*I*). *Error bars*, SEM; $n = 7$–9 per group. Analysis by two-way ANOVA with Bonferroni's multiple comparisons test. Ea, arterial elastance; EDPVR, end-diastolic pressure–volume relationship; Ees, end-systolic elastance; ESPVR, end-systolic pressure–volume relationship. $*P < 0.05$, $**P < 0.01$, $***P < 0.001$.

including mitochondrially encoded ND1 is typically preserved (27). Thus, to corroborate our finding of DNA damage, we analyzed the ratio of ND4:ND1 by PCR and identified that hyperoxia-exposed animals had significantly lower ND4:ND1 than controls (Figure 5C). Finally,

hyperoxia-exposed animals demonstrated a decrease in antioxidants, specifically superoxide dismutase 1 and 2 with findings again most notable in Hx-M, which could further predispose to or exacerbate oxidative stress (Figures 5D–5F).

Postnatal Hx Is not Associated with Impaired Autophagy or Enhanced Cardiac Fibrosis with Age

As mitochondrial dysfunction is frequently reported in cardiac aging (28–30), we evaluated alternative processes of accelerated cardiac aging after postnatal
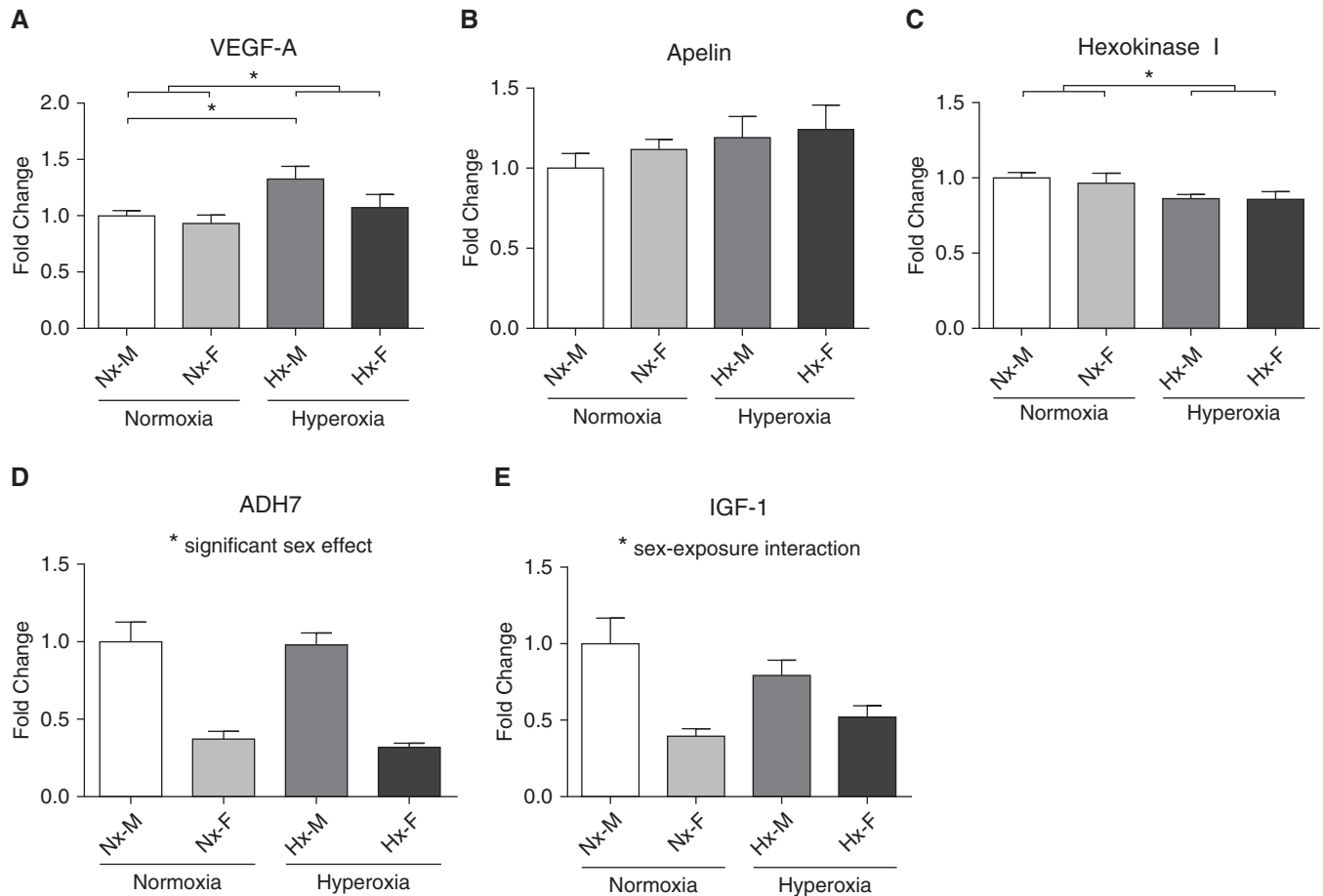
Figure 3. Chronic pressure overload from postnatal Hx results in up-regulation of a more adaptive RV hypertrophy gene panel. Despite significant RV dysfunction by invasive hemodynamics, there is a significant increase in vascular endothelial growth factor (A), nonsignificant increase in apelin (B), decrease in hexokinase 1 (C), and no hyperoxia-induced changes in alcohol dehydrogenase 7 (D) or insulin-like growth factor-1 (E) in the RV 1 year after postnatal Hx, a pattern most consistent with the gene profile seen in adaptive RV hypertrophy rather than RV failure. *Error bars*, SEM; $n = 6$ per group. Analysis by two-way ANOVA with Bonferroni's multiple comparisons test. ADH7, alcohol dehydrogenase 7; IGF-1, insulin-like growth factor 1; VEGF-A, vascular endothelial growth factor A. *$P < 0.05$.

Hx, including impaired autophagy or enhanced cardiac fibrosis. Analysis of key autophagy proteins, including beclin, p62, microtubule-associated protein light chain 3 I to II conversion, and lysosome-associated membrane protein 2, did not indicate alterations in RV autophagy after postnatal Hx (Figures 6A–6E). Furthermore, RV hydroxyproline content and Masson's trichrome scoring failed to identify increases in RV fibrosis (Figures 6F–6H), suggesting overt cardiac fibrosis was not the cause of impaired RV systolic or diastolic function.

Discussion

Postnatal Hx in rodents aged to 1 year, or roughly 30 human years, recapitulates

several of the known clinical features of young adults with a history of premature birth. Specifically, we identified increased body mass, increased RV mass, and a decreased RV ejection fraction in rats 1 year after postnatal Hx, consistent with clinical studies of adults born prematurely (10, 31). Our model was also characterized by chronic RV pressure overload due to hypertensive pulmonary vascular disease, as well as intrinsic RV dysfunction noted by the inability to maintain contractility in the setting of increased afterload.

To our knowledge, the current study represents the longest duration of RV pressure overload in an animal model. Intriguingly, the adaptive gene signaling profile previously identified by Drake and

colleagues (22) in shorter duration RV pressure overload states, including pulmonary artery banding, remains largely active in this model of chronic pressure overload. Given the predominately adaptive gene profile seen here, yet clear maladaptive features of decreased contractility and mitochondrial dysregulation, it is possible that the adaptive gene signaling profile that is protective in shorter duration models of pressure overload becomes "overwhelmed" by maladaptive features arising with longer-term chronic pressure overload. Alternatively, an intriguing hypothesis is that postnatal hyperoxia exerts a direct noxious effect on the developing RV, independent of that on the pulmonary vasculature, which persists or worsens with aging.
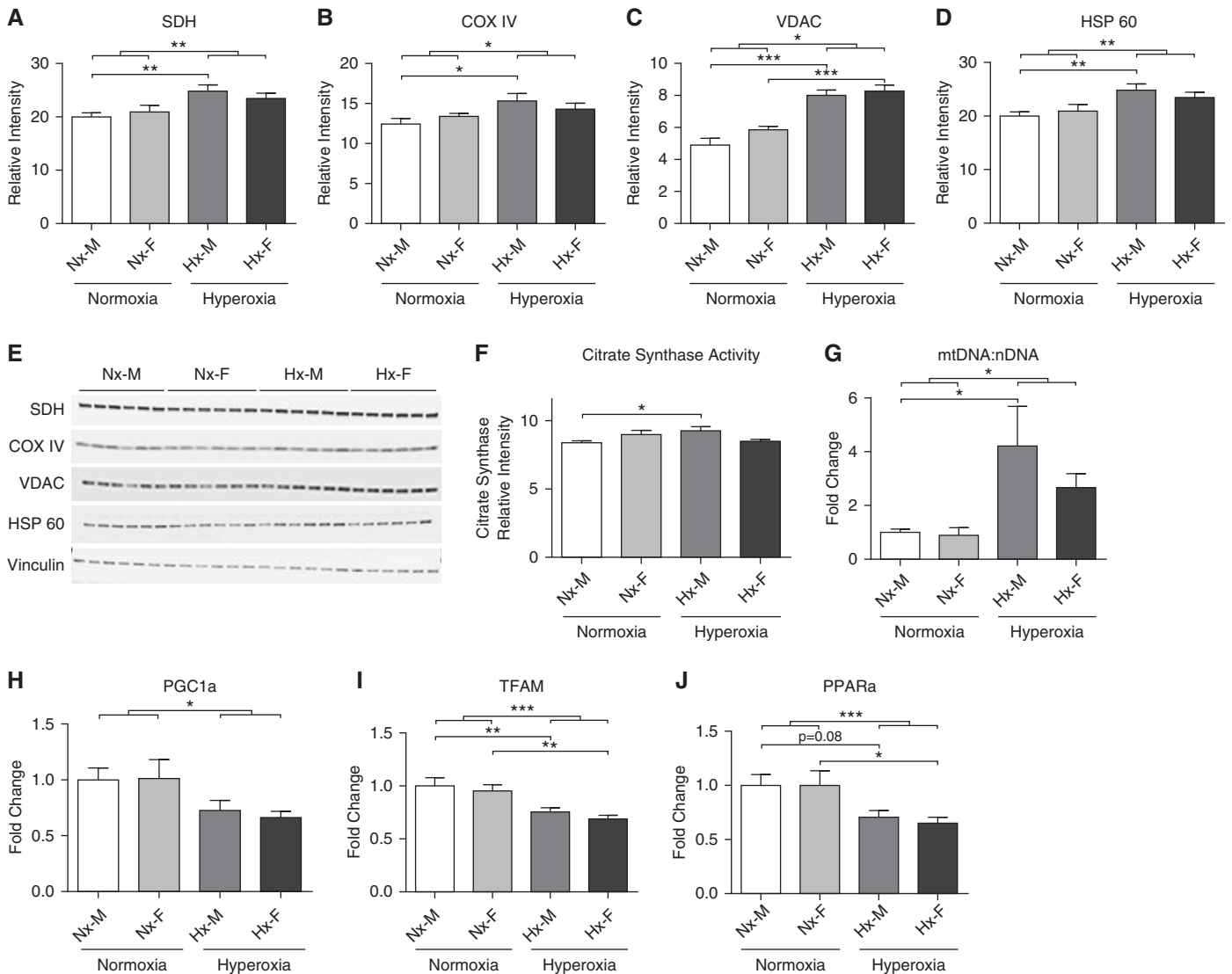
Figure 4. Postnatal Hx results in an increase in mitochondrial abundance but decreased biogenesis at 1 year. Western blotting demonstrates increased RV succinate dehydrogenase (SDH) (*A*), cytochrome c oxidase (COX) IV (*B*), voltage-dependent anion channel (*C*), and heat shock protein 60 (*D*) (normalized to vinculin) after Hx, all key elements of mitochondrial structure. Representative blots shown (*E*). An increase in mitochondrial abundance was also supported by increased citrate synthase activity assay in Hx-M (*F*) as well as an increased ratio of mitochondrial (mt) to nuclear (n) DNA in both Hx-M and Hx-F (*G*). At 1 year of age, mitochondrial biogenesis markers proliferator–activated receptor γ coactivator 1α (*H*), mitochondrial transcription factor A (*I*), and peroxisome proliferator–activated receptor-α (*J*) (assessed by RT-PCR) were all down-regulated after Hx, suggesting biogenesis is not maintained with age after neonatal Hx. *Error bars*, SEM; *n* = 6 per group. Analysis by two-way ANOVA with Bonferroni's multiple comparisons test. HSP, heat shock protein; PGC1a, peroxisome proliferator–activated receptor γ coactivator 1α; PPARα, peroxisome proliferator–activated receptor-α; TFAM, mitochondrial transcription factor A; VDAC, voltage-dependent anion channel. *$P < 0.05$, **$P < 0.01$, ***$P < 0.001$.

The presence of dysregulated mitochondrial dynamics identified in this study, including impaired mitochondrial biogenesis and mitochondrial DNA damage, may suggest a direct deleterious effect of prematurity and Hx on the RV. Clearly, a direct contribution from the coexisting pulmonary hypertension cannot be completely ruled out, as mitochondrial dysfunction and metabolic gene

reprogramming within the RV have previously been identified in animal models and humans with pulmonary arterial hypertension (32–34). However, these are typically models of RV failure, and mitochondrial dysfunction and impaired biogenesis were not demonstrated in the pulmonary artery banding model of chronic pressure overload (32), which appears more akin, in many ways, to the current postnatal Hx model. Thus, a

direct effect of hyperoxia on the immature RV cardiomyocyte should be considered. Although postnatal Hx is known to acutely worsen mitochondrial dysfunction and oxidative stress in the lung, relative hyperoxia, as is encountered at birth into a normoxic environment, is critical to initiate neonatal cardiac mitochondrial biogenesis and oxidative metabolism within the LV (35–38). However,
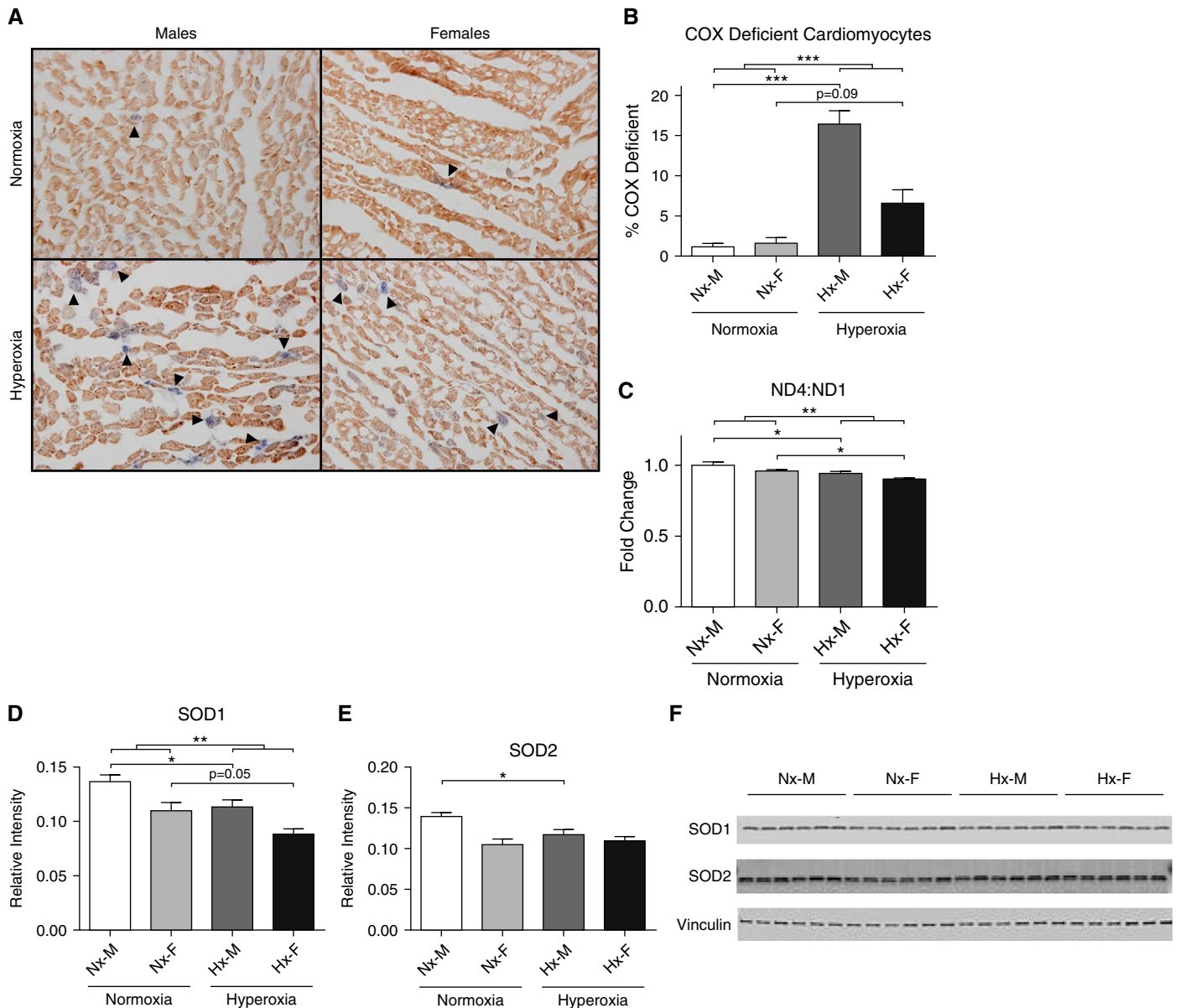
Figure 5. mtDNA damage accumulates in RV cardiomyocytes after postnatal Hx. COX/SDH co-staining demonstrates numerous functionally COX-deficient cardiac myocytes (*blue*, *arrowheads*) in hyperoxia-exposed animals, suggestive of accumulation of mtDNA damage (*A* and *B*). Increased DNA damage was confirmed by a decrease in the ratio of nicotinamide adenine dinucleotide$^+$ reduced dehydrogenase (ND) 4:ND1 in hyperoxia-exposed animals (*C*). In addition, hyperoxia-exposed animals have decreased antioxidants, superoxide dismutase (SOD) 1 and SOD2, which may predispose to further oxidant stress (*D–F*). Images at 40× magnification. *Error bars*, SEM; $n = 4$ per group for immunohistochemistry, 6 per group for PCR and Western blots. Analysis by two-way ANOVA with Bonferroni's multiple comparisons test. *$P < 0.05$, **$P < 0.01$, ***$P < 0.001$.

the acute and chronic effects of postnatal hyperoxia on the RV remain unknown.

The hallmark pathologic RV feature identified after postnatal Hx in this study was mitochondrial dysregulation, including decreased mitochondrial biogenesis and evidence of mitochondrial DNA damage, despite increased mitochondrial abundance. Importantly, this paradigm of altered

mitochondrial dynamics, including increased mitochondrial abundance, but decreased biogenesis, is frequently encountered in other forms of cardiomyopathy (23, 39). Early in disease in the compensated hypertrophy stage, there is an increase in mitochondrial biogenesis to maintain energy production, but this wanes over time. Whether biogenesis is up-regulated early in the

postnatal hyperoxia model remains to be determined.

The presence of COX$^-$/SDH$^+$ RV cardiomyocytes is highly suggestive of mitochondrial DNA damage, as the catalytic subunits of COX are encoded by mitochondrial DNA, and thus proper synthesis and function are predominately dependent on mitochondrial DNA integrity (19, 40). This finding is further
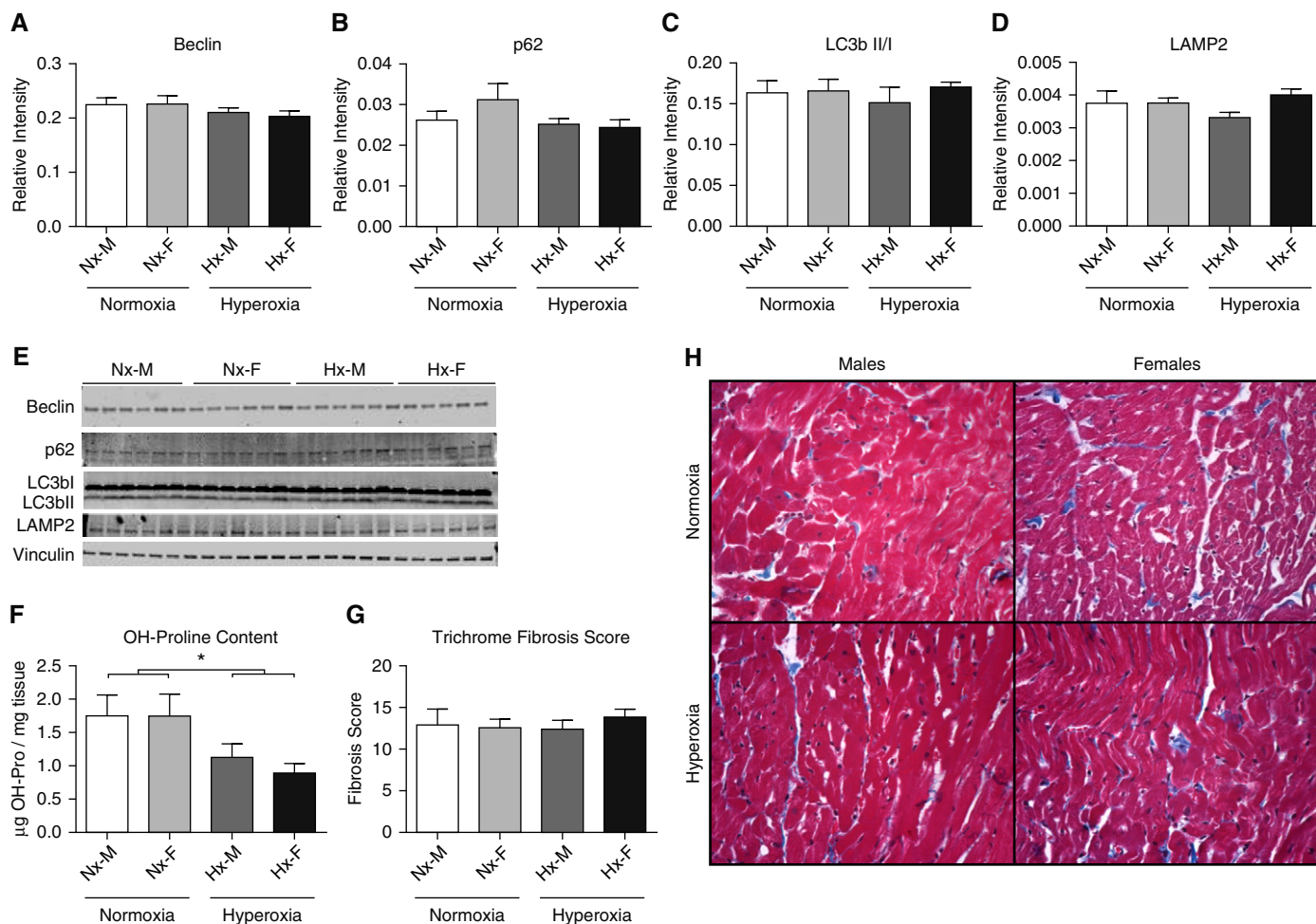
Figure 6. Postnatal Hx is not associated with other processes of accelerated aging, including impaired autophagy or enhanced RV fibrosis. Key autophagy proteins, including beclin (A), p62 (B), microtubule-associated protein light chain 3 (C), and lysosome-associated membrane protein 2 (D), were unchanged after postnatal Hx. Representative blots shown (E). Masson's trichrome staining for collagen failed to identify significant differences in RV fibrosis after postnatal hyperoxia (G and H), whereas measurements of hydroxyproline (OH-proline) were lower after neonatal Hx (F). *P < 0.05 for normoxia versus hyperoxia. Images at 40× magnification. Error bars, SEM; n = 4–7 per group for histology, 6 per group for Western blots and OH-proline content. Analysis by two-way ANOVA with Bonferroni's multiple comparisons test. LC3b, microtubule-associated protein light chain 3; LAMP2, lysosome-associated membrane protein 2.

corroborated by the decrease in ND4 relative to ND1, as ND4 is among the most frequently deleted areas of mitochondrial DNA. Interestingly, loss of mitochondrial DNA content has been shown to down-regulate modulators of mitochondrial biogenesis, beginning during RV hypertrophy and progressing further with the onset of RV failure (41, 42). Complete loss of COX activity has previously been suggested to occur when mutation abundance surpasses 90% of the total mitochondrial genome (26), which would suggest a relatively high burden of mitochondrial DNA damage in Hx animals, particularly males. Surprisingly, we did not identify other features of accelerated cardiac aging in this model,

including autophagy and fibrosis, although autophagy is a very dynamic process, and alterations there cannot be fully ruled out.

The finding that males appear to be more affected in this model may be clinically significant. First, male neonates born premature are more likely to develop bronchopulmonary dysplasia, and more likely to have severe disease (43). Second, strong sex differences also exist among patients with pulmonary hypertension and RV dysfunction, and, although females are more likely to develop pulmonary hypertension, males who do develop the disease have a more severe course (44). Interestingly, numerous studies have identified decreased antioxidant enzymes

and increased reactive oxygen species production in males compared with females (45, 46), which may have contributed to the sex-specific findings in this study.

Strengths of the current study include the detailed physiologic assessments, clinically relevant long-term nature of the study, and the evaluation of sex as an independent variable. There are limitations to the indirect measures of mitochondrial abundance and function employed in this study, and direct measures of mitochondrial function, including mitochondrial respiration and production of reactive oxygen species, as well as mitochondrial structure by electron microscopy, merits further

evaluation and is the subject of ongoing investigations in our laboratory. In addition, some of our findings were modest in this aged model, but could be more notable in younger animals or in animals with overt RV failure.

In summary, we have recapitulated the known RV phenotype of human young adults born prematurely, and, in addition, have identified unique alterations in RV mitochondrial regulation in a rodent model of postnatal

Hx aged to the equivalent of young to middle-aged adulthood. Our findings of mitochondrial dysregulation may explain, at least in part, the decreased RV function noted in young adults born prematurely. In particular, the findings of mitochondrial DNA damage and dysregulated biogenesis could have significant implications to the thousands of young adults born prematurely, increasing their risk for long-term RV dysfunction, failure, and, ultimately, premature death. Further studies

investigating mitochondrial deficiency and dysfunction in early and late time points in both animal models and humans born preterm are warranted. ∎

References

1. U.S. Department of Health and Human Services, Health Resources and Services Administration, Maternal and Child Health Bureau. Child Health USA 2013. Rockville, MD: U.S. Department of Health and Human Services, 2013.
2. Gough A, Spence D, Linden M, Halliday HL, McGarvey LPA. General and respiratory health outcomes in adult survivors of bronchopulmonary dysplasia: a systematic review. *Chest* 2012;141: 1554–1567.
3. Bates ML, Farrell ET, Eldridge MW. Abnormal ventilatory responses in adults born prematurely. *N Engl J Med* 2014;370:584–585.
4. Islam JY, Keller RL, Aschner JL, Hartert TV, Moore PE. Understanding the Short- and Long-Term Respiratory Outcomes of Prematurity and Bronchopulmonary Dysplasia. *Am J Respir Crit Care Med* 2015;192: 134–156.
5. Parkinson JR, Hyde MJ, Gale C, Santhakumaran S, Modi N. Preterm birth and the metabolic syndrome in adult life: a systematic review and meta-analysis. *Pediatrics* 2013;131:e1240–e1263.
6. Sipola-Leppänen M, Vääräsmäki M, Tikanmäki M, Matinolli HM, Miettola S, Hovi P, Wehkalampi K, Ruokonen A, Sundvall J, Pouta A, et al. Cardiometabolic risk factors in young adults who were born preterm. *Am J Epidemiol* 2015;181:861–873.
7. Abitbol CL, Rodriguez MM. The long-term renal and cardiovascular consequences of prematurity. *Nat Rev Nephrol* 2012;8:265–274.
8. Lewandowski AJ, Augustine D, Lamata P, Davis EF, Lazdam M, Francis J, McCormick K, Wilkinson AR, Singhal A, Lucas A, et al. Preterm heart in adult life: cardiovascular magnetic resonance reveals distinct differences in left ventricular mass, geometry, and function. *Circulation* 2013;127:197–206.
9. Naumburg E, Axelsson I, Huber D, Söderström L. Some neonatal risk factors for adult pulmonary arterial hypertension remain unknown. *Acta Paediatr* 2015;104:1104–1108.
10. Lewandowski AJ, Bradlow WM, Augustine D, Davis EF, Francis J, Singhal A, Lucas A, Neubauer S, McCormick K, Leeson P. Right ventricular systolic dysfunction in young adults born preterm. *Circulation* 2013;128:713–720.
11. O'Reilly M, Thébaud B. Animal models of bronchopulmonary dysplasia: the term rat models. *Am J Physiol Lung Cell Mol Physiol* 2014;307: L948–L958.
12. Botting KJ, Wang KCW, Padhee M, McMillen IC, Summers-Pearce B, Rattanatray L, Cutri N, Posterino GS, Brooks DA, Morrison JL. Early origins of heart disease: low birth weight and determinants of cardiomyocyte endowment. *Clin Exp Pharmacol Physiol* 2012;39: 814–823.
13. Yee M, White RJ, Awad HA, Bates WA, McGrath-Morrow SA, O'Reilly MA. Neonatal hyperoxia causes pulmonary vascular disease and shortens life span in aging mice. *Am J Pathol* 2011;178: 2601–2610.
14. Ventetuolo CE, Ouyang P, Bluemke DA, Tandri H, Barr RG, Bagiella E, Cappola AR, Bristow MR, Johnson C, Kronmal RA, et al. Sex hormones are associated with right ventricular structure and function: the MESA–right ventricle study. *Am J Respir Crit Care Med* 2011;183:659–667.
15. Kumar VH, Hutchison AA, Lakshminrusimha S, Morin FC III, Wynn RJ, Ryan RM. Characteristics of pulmonary hypertension in preterm neonates. *J Perinatol* 2007;27:214–219.
16. Goss KN, Tetri LH, Haraldsdottir K, Braun RK, Hacker TA, Eldridge MW. Postnatal hyperoxia exposure durably impairs right ventricular function in aged male rats [abstract]. *Am J Respir Crit Care Med* 2016;193:A3880.
17. Hacker TA, McKiernan SH, Douglas PS, Wanagat J, Aiken JM. Age-related changes in cardiac structure and function in Fischer 344 × brown Norway hybrid rats. *Am J Physiol Heart Circ Physiol* 2006;290: H304–H311.
18. Tabima DM, Hacker TA, Chesler NC. Measuring right ventricular function in the normal and hypertensive mouse hearts using admittance-derived pressure–volume loops. *Am J Physiol Heart Circ Physiol* 2010;299:H2069–H2075.
19. Ross JM. Visualization of mitochondrial respiratory function using cytochrome c oxidase/succinate dehydrogenase (COX/SDH) double-labeling histochemistry. *J Vis Exp* 2011;(57):e3266.
20. Goss KN, Cucci AR, Fisher AJ, Albrecht M, Frump A, Tursunova R, Gao Y, Brown MB, Petrache I, Tepper RS, et al. Neonatal hyperoxic lung injury favorably alters adult right ventricular remodeling response to chronic hypoxia exposure. *Am J Physiol Lung Cell Mol Physiol* 2015;308: L797–L806.
21. Farriol M, Rosselló J, Schwartz S. Body surface area in Sprague-Dawley rats. *J Anim Physiol Anim Nutr (Berl)* 1997;77:61–65.
22. Drake JI, Bogaard HJ, Mizuno S, Clifton B, Xie B, Gao Y, Dumur CI, Fawcett P, Voelkel NF, Natarajan R. Molecular signature of a right heart failure program in chronic severe pulmonary hypertension. *Am J Respir Cell Mol Biol* 2011;45:1239–1247.
23. Rosca MG, Hoppel CL. Mitochondrial dysfunction in heart failure. *Heart Fail Rev* 2013;18:607–622.
24. Jonas EA, Hickman JA, Chachar M, Polster BM, Brandt TA, Fannjiang Y, Ivanovska I, Basañez G, Kinnally KW, Zimmerberg J, et al. Proapoptotic N-truncated BCL-xL protein activates endogenous mitochondrial channels in living synaptic terminals. *Proc Natl Acad Sci USA* 2004;101:13590–13595.
25. Capaldi RA, Murray J, Byrne L, Janes MS, Marusich MF. Immunological approaches to the characterization and diagnosis of mitochondrial disease. *Mitochondrion* 2004;4:417–426.
26. Herbst A, Pak JW, McKenzie D, Bua E, Bassiouni M, Aiken JM. Accumulation of mitochondrial DNA deletion mutations in aged muscle fibers: evidence for a causal role in muscle fiber loss. *J Gerontol A Biol Sci Med Sci* 2007;62:235–245.
27. Kowald A, Kirkwood TBL. Transcription could be the key to the selection advantage of mitochondrial deletion mutants in aging. *Proc Natl Acad Sci USA* 2014;111:2972–2977.
28. Moslehi J, DePinho RA, Sahin E. Telomeres and mitochondria in the aging heart. *Circ Res* 2012;110:1226–1237.
29. Dai DF, Rabinovitch PS, Ungvari Z. Mitochondria and cardiovascular aging. *Circ Res* 2012;110:1109–1124.
30. Dutta D, Calvani R, Bernabei R, Leeuwenburgh C, Marzetti E. Contribution of impaired mitochondrial autophagy to cardiac aging: mechanisms and therapeutic opportunities. *Circ Res* 2012;110: 1125–1138.

31. Hui LL, Lam HS, Leung GM, Schooling CM. Late prematurity and adiposity in adolescents: evidence from "Children of 1997" birth cohort. *Obesity (Silver Spring)* 2015;23:2309–2314.

32. Gomez-Arroyo J, Mizuno S, Szczepanek K, Van Tassell B, Natarajan R, dos Remedios CG, Drake JI, Farkas L, Kraskauskas D, Wijesinghe DS, *et al*. Metabolic gene remodeling and mitochondrial dysfunction in failing right ventricular hypertrophy secondary to pulmonary arterial hypertension. *Circ Heart Fail* 2013;6:136–144.

33. Balestra GM, Mik EG, Eerbeek O, Specht PA, van der Laarse WJ, Zuurbier CJ. Increased *in vivo* mitochondrial oxygenation with right ventricular failure induced by pulmonary arterial hypertension: mitochondrial inhibition as driver of cardiac failure? *Respir Res* 2015;16:6.

34. Piao L, Marsboom G, Archer SL. Mitochondrial metabolic adaptation in right ventricular hypertrophy and failure. *J Mol Med (Berl)* 2010;88:1011–1020.

35. Berkelhamer SK, Kim GA, Radder JE, Wedgwood S, Czech L, Steinhorn RH, Schumacker PT. Developmental differences in hyperoxia-induced oxidative stress and cellular responses in the murine lung. *Free Radic Biol Med* 2013;61:51–60.

36. Das KC. Hyperoxia decreases glycolytic capacity, glycolytic reserve and oxidative phosphorylation in MLE-12 cells and inhibits complex I and II function, but not complex IV in isolated mouse lung mitochondria. *PLoS One* 2013;8:e73358.

37. McGrath-Morrow S, Lauer T, Yee M, Neptune E, Podowski M, Thimmulappa RK, O'Reilly M, Biswal S. Nrf2 increases survival and attenuates alveolar growth inhibition in neonatal mice exposed to hyperoxia. *Am J Physiol Lung Cell Mol Physiol* 2009;296:L565–L573.

38. Neary MT, Ng K-E, Ludtmann MHR, Hall AR, Piotrowska I, Ong S-B, Hausenloy DJ, Mohun TJ, Abramov AY, Breckenridge RA. Hypoxia signaling controls postnatal changes in cardiac mitochondrial morphology and function. *J Mol Cell Cardiol* 2014;74:340–352.

39. Ahuja P, Wanagat J, Wang Z, Wang Y, Liem DA, Ping P, Antoshechkin IA, Margulies KB, Maclellan WR. Divergent mitochondrial biogenesis responses in human cardiomyopathy. *Circulation* 2013;127: 1957–1967.

40. Cottrell DA, Blakely EL, Borthwick GM, Johnson MA, Taylor GA, Brierley EJ, Ince PG, Turnbull DM. Role of mitochondrial DNA mutations in disease and aging. *Ann N Y Acad Sci* 2000;908: 199–207.

41. Pisano A, Cerbelli B, Perli E, Pelullo M, Bargelli V, Preziuso C, Mancini M, He L, Bates MGD, Lucena JR, *et al*. Impaired mitochondrial biogenesis is a common feature to myocardial hypertrophy and end-stage ischemic heart failure. *Cardiovasc Pathol* 2016;25: 103–112.

42. Karamanlidis G, Bautista-Hernandez V, Fynn-Thompson F, Del Nido P, Tian R. Impaired mitochondrial biogenesis precedes heart failure in right ventricular hypertrophy in congenital heart disease. *Circ Heart Fail* 2011;4:707–713.

43. Trembath A, Laughon MM. Predictors of bronchopulmonary dysplasia. *Clin Perinatol* 2012;39:585–601.

44. Austin ED, Lahm T, West J, Tofovic SP, Johansen AK, Maclean MR, Alzoubi A, Oka M. Gender, sex hormones and pulmonary hypertension. *Pulm Circ* 2013;3:294–314.

45. Borrás C, Sastre J, García-Sala D, Lloret A, Pallardó FV, Viña J. Mitochondria from females exhibit higher antioxidant gene expression and lower oxidative damage than males. *Free Radic Biol Med* 2003;34:546–552.

46. Viña J, Borrás C, Gambini J, Sastre J, Pallardó FV. Why females live longer than males? Importance of the upregulation of longevity-associated genes by oestrogenic compounds. *FEBS Lett* 2005;579: 2541–2545.